Biogeosciences Discussions, 1, 561–589, 2004
www.biogeosciences.net/bgd/1/561/
SRef-ID: 1810-6285/bgd/2004-1-561

Biogeosciences Discussions

Biogeosciences Discussions is the access reviewed discussion forum of *Biogeosciences*

Carbon dynamics and CO_2 air-sea exchanges in the eutrophied coastal waters of the southern bight of the North Sea: a modelling study

N. Gypens[1], C. Lancelot[1], and A. V. Borges[2]

[1]Université Libre de Bruxelles, Ecologie des Systèmes Aquatiques, CP-221, Bd du Triomphe, B-1050, Belgium
[2]Université de Liège, MARE, Unité d'Océanographie Chimique, Institut de Physique (B5), B-4000 Sart Tilman, Belgium

Received: 16 August 2004 – Accepted: 22 August 2004 – Published: 7 September 2004

Correspondence to: N. Gypens (ngypens@ulb.ac.be)

Abstract

A description of the carbonate system has been incorporated in the MIRO biogeochemical model to investigate the contribution of diatom and Phaeocystis blooms to the seasonal dynamics of air-sea CO_2 exchanges in the Eastern Channel and Southern Bight of the North Sea with focus on the eutrophied Belgian coastal waters. For this application the model was implemented in a simplified three-box representation of the hydrodynamics including the open ocean boundary box 'Western English Channel' (WCH) and the 'French Coastal Zone' (FCZ) and 'Belgian Coastal Zone' (BCZ) boxes receiving carbon and nutrients from the rivers Seine and Scheldt, respectively. Results were obtained by running the model for the 1996–1999 period. The predicted partial pressures of CO_2 (pCO_2) were successfully compared with data recorded over the same period in the central BCZ at station 330 (51°26.05′ N; 002°48.50′ E). Budget calculations based on model simulations of carbon flow rates indicated for BCZ a low annual sink of atmospheric CO_2 (-0.17 mol C m^{-2} y^{-1}). On the opposite surface water pCO_2 in WCH was estimated in annual equilibrium with respect to atmospheric CO_2. The relative contribution of biological, chemical and physical processes to the modelled pCO_2 seasonal variability in BCZ was further explored by running model scenarios with separate closures of biological activities and carbon rivers inputs. The suppression of biological processes reversed direction of the CO_2 flux in BCZ that became, on an annual scale, a significant source for atmospheric CO_2 ($+0.58$ mol C m^{-2} y^{-1}). Overall biological activity had a stronger influence on the modelled seasonal cycle of pCO_2 than temperature. Especially Phaeocystis colonies which spring growth was associated with an important sink of atmospheric CO_2 that counteracted the temperature-driven increase of pCO_2 in spring. On the other hand, river inputs of organic and inorganic carbon were shown to increasing water pCO_2 and hence emission of CO_2 to the atmosphere. Same calculations conducted in WCH, showed that temperature was the main factor controlling the seasonal pCO_2 cycle in these waters. The effect of interannual variations of fresh water discharge (and related nutrient and carbon inputs), tempera-

ture and wind speed was further explored by running scenarios with forcings typical of two contrasted years (1996 and 1999). Based on these simulations, the model predicts significant variations in the intensity and direction of the annual air-sea CO_2 flux.

1 Introduction

Coastal waters are heavily impacted by nutrients, and inorganic and organic carbon inputs from rivers and estuaries. They also intensively exchange nutrients, and inorganic and organic carbon with the open ocean across marginal boundaries (e.g. Thomas et al., 2004a). Consequently, these areas play a key role in the global carbon cycle through production and remineralization of organic matter (Gattuso et al., 1998; Mackenzie et al., 2004). However, there is yet a great uncertainty on the geographical and ecological variability of air-sea CO_2 exchanges and the overall role as a sink or a source for atmospheric CO_2 played by these coastal areas. Existing data of CO_2 air-sea fluxes suggest that temperate marginal seas act as sinks for atmospheric CO_2 (Tsunogai et al., 1999; Frankignoulle and Borges, 2001a; Borges and Frankignoulle, 2002a; DeGranpre et al., 2002; Thomas et al., 2004a, b). On the contrary sub-tropical marginal seas (Cai et al., 2003) and near-shore ecosystems influenced by terrestrial inputs such as inner and outer estuaries (Frankignoulle et al., 1998; Cai et al., 2000; Raymond et al., 2000; Borges and Frankignoulle 2002b; Bouillon et al., 2003), mangroves (Borges et al., 2003) and non-estuarine salt marshes (Wang and Cai, 2004) act as sources of CO_2 to the atmosphere. However, the paucity of field data prevents the comprehensive description of the geographical and ecological diversity of coastal ecosystems and the integration of CO_2 fluxes on a global scale. Furthermore, little is known on the interannual variability of CO_2 dynamics and fluxes in coastal ecosystems, although it has been shown to be highly significant in open oceanic waters in relation to large scale climatic forcings acting at various time-scales (e.g. Takahashi et al., 2002, 2003). In the absence of long term time-series, these aspects of CO_2 cycling in coastal ecosystems can only be approached with modelling tools (e.g. Ianson

and Allen, 2002). However, very few mechanistic modelling efforts have been made to describe the dynamics of dissolved inorganic carbon (DIC) in coastal environments (Walsh et al., 1994, 1996; Mackenzie et al., 2004).

The North Sea is amongst the best-studied coastal areas in the World, with respect to its physical, chemical and biological characteristics. However, the monitoring of the DIC spatio-temporal variability has been limited to near-shore waters such as the German Bight, the Wadden Sea or the Belgian coastal zone (Hoppema, 1991; Borges and Frankignoulle, 1999, 2002b; Brasse et al., 2002). Recently the seasonality of pCO_2 has been investigated in the whole North Sea (Thomas et al., 2004b). On this basis a detailed carbon budget that identifies the major players in the large scale air-sea CO_2 fluxes has been established (Thomas et al., 2004b). Results point the Southern Bight as distinct from the Northern North Sea in terms of organic and inorganic carbon cycling. This is related to both their different hydrographic features (permanently well-mixed versus seasonally-stratified water column, in the South and North, respectively) and the influence of rivers inputs that are concentrated in the Southern Bight.

The Belgian coastal zone (BCZ) localised in the Southern Bight of the North Sea is a highly dynamic system with water masses resulting from the variable mixing between the inflowing southwest Atlantic waters through the Strait of Dover and the Scheldt freshwater and nutrient inputs. The inflowing Atlantic waters are themselves enriched with nutrient inputs from the river Seine (Lancelot et al., 1987). The river inputs characterized by a large excess of nitrate over phosphate and silicate are shaping the structure and the functioning of the ecosystem characterized by the dominance of undesirable recurrent non-siliceous phytoplankton like *Phaeocystis* colonies (Lancelot, 1995).

In this paper, we test a complex biogeochemical model (MIRO-CO_2) to investigate the present-day impact of land-based nutrients and carbon inputs from the Seine and Scheldt rivers on the functioning of the *Phaeocystis*-dominated ecosystem of the Southern Bight of the North Sea and the related air-sea CO_2exchanges. The model is run over the 1996–1999 period when existing data of CO_2 partial pressure (pCO_2)

allow model validation. We further conduct model scenarios to evaluate the respective contribution of biological, chemical and physical processes to the seasonal and annual variability of pCO_2. Finally, we investigate the impact of the main model external forcings (river inputs, temperature, wind stress) on the pCO_2 dynamics by running scenarios with contrasted but realistic meteorological conditions.

2 Material and method

2.1 Model description

The MIRO-CO_2 biogeochemical model results of the coupling to the complex biogeochemical MIRO model (Lancelot et al., in review, 2004[1]) of the physico-chemical module of Hannon et al. (2001) describing the seawater carbonate system and air-sea CO_2 exchange. MIRO is a mechanistic model that describes C, N, P and Si cycling through aggregated components of the *Phaeocystis*-dominated ecosystem of the North Sea. It includes thirty-two state variables assembled in four modules describing the dynamics of phytoplankton (diatoms, nanoflagellates and *Phaeocystis*), zooplankton (copepods and microzooplankton), organic matter degradation and nutrients (NO_3, NH_4, PO_4 and SiO), regeneration by bacteria in the water column and the sediment. The degradation of organic matter by planktonic bacteria is described considering two classes of biodegradability for both dissolved and particulate organic matter (Billen and Servais, 1989). Conservation equations and parameters are detailed in Lancelot et al. (in review, 2004[1]).

The physico-chemical module of Hannon et al. (2001) describes the carbonate system in seawater and calculates CO_2 exchange between the surface water and the low

[1] Lancelot, C., Spitz, Y., Gypens, N., Ruddick, K., Becquevort, S., Rousseau, V., Lacroix, G., and Billen, G.: Modelling diatom-*Phaeocystis* blooms and nutrient cycles in the Southern Bight of the North Sea with focus on the Belgian coastal zone: the MIRO model, Mar. Ecol. Prog. Syst., in review, 2004.

atmosphere. The speciation of the carbonate system (in particular pCO_2) is calculated based on the knowledge of only DIC and total alkalinity (TA), using stoichiometric relationships and apparent equilibrium constants, which are function of temperature, pressure and salinity (Weiss, 1974; Millero et al., 1993). DIC and TA are computed taking into account, respectively, the biological uptake or release of carbon and nitrate calculated by the MIRO model. Air-sea CO_2 fluxes are calculated from the pCO_2 gradient across the air-sea interface and the gas transfer velocity computed from wind speed using the parameterisation of Nightingale et al. (2000). The latter was chosen among several existing empirical formulations since it was established from dual tracer experiments in the Southern Bight of the North Sea.

2.2 Model runs

The MIRO-CO_2 model was applied in the coastal domain of the eastern Channel and Southern Bight of the North Sea, between the Baie de Seine and the northern limit of BCZ (Fig. 1). The model was implemented in a multi-box frame delineated on the basis of hydrological regime and river inputs. In order to take into account the cumulated nutrient enrichment of Atlantic waters by the Seine and Scheldt rivers, two successive boxes, assumed to be homogeneous, were chosen from the Baie de Seine to the BCZ (Fig. 1). Each box was characterized by its own area, depth, water temperature, light conditions and water residence time and was treated as an open system, receiving water from the upward adjacent box and exporting water to the downward box (Lancelot et al., in review, 2004[1]). The seasonal variation of the state variables was calculated by solving the equations expressing mass conservation, according to the Euler procedure, with a time step of 15 min. The South-Western boundary conditions were provided by the results of MIRO calculations performed for the conditions existing in the western Channel area (WCH), considered as a quasi oceanic closed system (no river input).

Model simulations were run with 1996–1999 climatological forcings for hydrometeorological conditions and river inputs. These functions were computed from recorded daily global solar radiation (Oostende Station, Institut Royal de Météorologie,

Belgium), seawater temperature and monthly nutrient loads for the rivers Seine (Cellule Antipollution de Rouen du Service de la Navigation de la Seine, France) and Scheldt ((Institute for Inland Water Management and Waste Water Treatment, The Netherlands) and Department of Environment and Infrastructure (Ministry of Flemish Community, Belgium)). Organic carbon loads by the Scheldt were retrieved from the Dutch water base (http://www.waterbase.nl). For the river Seine, we used data described in Servais et al. (2003). Land-based fluxes of DIC and alkalinity were estimated based on a compilation of DIC and TA data in the Seine and the Scheldt rivers (Frankignoulle et al., 1996, 1998; Frankignoulle and Borges, 2001b; Abril, personal communication) and river discharges, making use of the "apparent zero end-member" method (Kaul and Froelich, 1984). Atmospheric pCO_2 was extracted from the Mace Head (53°33′ N 9°00′ W, Southern Ireland) and the National Oceanic and Atmospheric Administration/climate Monitoring and Diagnostics Laboratory/Carbon Cycle Greenhouse Gases Group (NOAA/CMDL/CCGG) air sampling network (available at http://www.cmdl.noaa.gov/). Wind speed at 50.0° N 6.0° W was computed by the Pacific Fisheries Environmental Laboratory (PFEL) based on Fleet Numerical Meteorology and Oceanography Center (FNMOC) synoptic pressure fields.

2.3 Validation data

Model results were daily-averaged and compared with available data sets in the central BCZ at the station 330 (51°26.05 N; 02°48.50 E) for the 1996–1999 period. Over this period, temperature, nutrients, phytoplankton and chlorophyll data were collected at a weekly frequency except during winter when bimonthly (Rousseau, 2000). DIC was calculated from TA and pCO_2 measured between 1996 and 1999 in the BCZ and WCH (Borges and Frankignoulle, 1999, 2002b, 2003). Due to inherent discrepancy between actual field temperature and that imposed by the climatological forcings applied to the model, pCO_2field data were adjusted to the modelled temperature. In the same direction, DIC and TA field data were normalized to the mean salinity (33.5) of the reference

station 330 to overcome the effect of salinity.

3 Results and discussion

3.1 Model validation

3.1.1 Biological state variables

Figure 2 compares MIRO-CO_2 predictions of diatom (Fig. 2a) and *Phaeocystis* (Fig. 2b) biomass, total phytoplankton (mg Chl *a* m^{-3}, Fig. 2c), bacteria (Fig. 2d), microzooplanktonic (Fig. 2e) and copepods (Fig. 2f) biomass with field data collected between 1996 and 1999. The model describes reasonably well the main trends (timing and magnitude) of the diatom-*Phaeocystis*-diatom succession: spring diatoms (Fig. 2a) initiate the phytoplankton bloom in early March and are followed by *Phaeocystis* colonies (Fig. 2b) which reach concentrations of 20 mg Chl *a* m^{-3} in April (Fig. 2c). Summer diatoms develop after *Phaeocystis* decline and maintain up to fall. In agreement with observations, MIRO-CO_2 results show non-negligible concentration of diatoms all over the year (Fig. 2a) contrasting with the unique bloom of *Phaeocystis* in spring (Fig. 2b). Phytoplankton decline in spring stimulates the development of diverse heterotrophs such as bacteria (Fig. 2d), microzooplankton (Fig. 2e) and copepods (Fig. 2f). The seasonal succession and magnitude of spring bacteria and microzooplankton biomass are well captured by the model. However, biomass reached by copepods and bacteria in spring and fall respectively, are not properly simulated. Such failure of the model is discussed in Lancelot et al. (in review, 2004[1]) and is mainly attributed to some mismatch between the simulated seasonal succession of copepods and preys which might be related to unreliable description of the mortality process and fate of *Phaeocystis* colonies and derived matter as well as of the copepod feeding function. Experimental work in these matters is in progress.

3.1.2 Carbonate chemistry

Figure 3 compares MIRO-CO_2 simulations of $DIC_{(33.5)}$ (Fig. 3a), $TA_{(33.5)}$ (Fig. 3b) and pCO_2 (Fig. 3c) with field observations. The seasonal evolution of $DIC_{(33.5)}$ is quite well captured by the model but concentrations obtained slightly overestimate field data (~6%; Fig. 3a). Highest $DIC_{(33.5)}$ concentration is modelled during winter when auto- and hetero- biomass are low (Figs. 2, 3a). The simulated $DIC_{(33.5)}$ clearly reaches lowest values at the time of *Phaeocystis* bloom maximum (Figs. 2b, 3a) and increases in mid-May when heterotrophs prevail over autotrophs (Figs. 3a, 2d, e, f). The observed seasonal signal of $TA_{(33.5)}$ is well reproduced (Fig. 3b) but the modelled amplitude (110 mmol m^{-3}) is weak compared to that suggested by field data (~200 mmol m^{-3}, Fig. 3b). MIRO-CO_2 values of $TA_{(33.5)}$ are similar to field data in spring and summer although in the higher range but are systematically overestimated in fall and winter. Highest $TA_{(33.5)}$ concentration (Fig. 3a) is modelled in end April-early May when phytoplankton biomass is the highest (Fig. 2a, b, c) and decreases after until late fall (Fig. 3b). The comparison between modelled and measured pCO_2(Fig. 3c) shows that our model is able to reproduces quite well the seasonal variability, both in timing and amplitude. The latter (defined as the difference between the maximum and minimum values) is evaluated 300 ppm with pCO_2 values ranging between 445 ppm in summer and 145 ppm in spring (Fig. 3c). Model pCO_2 values generally agree fairly well with observations except in fall when field data are higher than modelled values. Over the winter season, modelled surface pCO_2 are close to saturation (Fig. 3c). A marked decrease of pCO_2 is simulated in early March and coincides with the onset of the diatom bloom (Figs. 3c, 2a) and pCO_2 reaches its minimum (145 ppm) during the *Phaeocystis* bloom (Figs. 3c, 2b). Modelled pCO_2 increases at *Phaeocystis* decline, reaching in July and up to end-October super-saturation values with respect to atmospheric CO_2 (Fig. 3c). In September and October, the model underestimates observed pCO_2. This could result from the underestimation of modelled bacterial biomass during fall (Fig. 2d).

3.2 Physical and biological control of pCO_2 and air-sea CO_2 fluxes in central BCZ at the seasonal and annual scale

Physical and biological mechanisms regulating pCO_2 (Fig. 3c) and air-sea CO_2 exchanges (Fig. 4a) in central BCZ were first investigated based on the comparative analysis of MIRO-CO_2 daily forcing of temperature (Fig. 4b) and predictions of biological features (gross primary production GPP, community respiration R (including autotrophic and heterotrophic planktonic and benthic respiration) and net ecosystem production NEP (the difference between GPP and R), Fig. 4c). In winter time (November to late February), NEP and R are close to zero (Fig. 4c) and pCO_2 mainly varies according to carbon river inputs and seawater temperature (Figs. 3c, 4b). The system is in equilibrium and air-sea CO_2 fluxes are close to zero (Fig. 4a). From mid-March to end April, NEP is high enough to reverse the positive effect of temperature increase on pCO_2 that reaches extremely low values with respect to saturation (Figs. 3c, 4b, c). In accordance our model calculates for this period an important sink of atmospheric CO_2 in central BCZ (Fig. 4a). In May, NEP is strongly negative (i.e. the system is heterotrophic) and surface water pCO_2 increases due to both respiration and temperature increase (Figs. 3c, 4b, c). As a consequence the system evolves progressively from a sink with respect to atmospheric CO_2 up to end-June towards a source until November (Fig. 4a). Overall MIRO-CO2 predicts an annual sink of atmospheric CO_2 of −0.17 mol C m^{-2} y^{-1}.

As a first attempt, to appraise the relative importance of physical and biological controls of surface water pCO_2, we used the approach of Takahashi et al. (2002) that separates the seasonal effect of biology from that of temperature. Removal of the temperature effect on pCO_2 is obtained after normalization of modelled daily values of pCO_2 to the annual mean temperature (11.9°C) using the equation:

$$pCO_2 \quad \text{at} \quad T_{mean} = pCO_{2\text{mod}} \cdot \exp\left[0.0423 \cdot (T_{mean} - T_{\text{mod}})\right], \tag{1}$$

where T_{mean} and T_{mod} are, respectively, the annual mean and modelled temperature in °C.

The seasonal effect of temperature on pCO_2 is estimated by attributing to the mean annual pCO_2 value of 360 ppm a correction factor based on the difference between the mean and modelled temperatures as follows:

$$pCO_2 \quad \text{at} \quad T_{\text{mod}}=\text{Mean annual } pCO_2 \cdot \exp\left[0.0423 \cdot (T_{\text{mod}} - T_{mean})\right] \tag{2}$$

According to this, the effect of biology on pCO_2, represented by the seasonal amplitude of pCO_2 values corrected to the mean annual temperature, is estimated at 350 ppm (150 ppm in May to 500 ppm in February). The effect of temperature change is less, 230 ppm (260 ppm in January–February to 490 ppm in July–August).

The relative importance of the temperature and biology effect (T/B) is derived from:

$$T/B = (\Delta pCO_2)_{temp} / (\Delta pCO_2)_{bio} = 0.66 \tag{3}$$

Thus, based on MIRO-CO_2 results we conclude that temperature contributed less to the seasonal pCO_2 variability of central BCZ in 1996–1999 than biological processes. However in areas influenced by river inputs of carbon and nutrients such as BCZ, the Takahashi et al. (2002) approach includes their impact in the estimation of biological contribution.

As an alternate approach to resolve these contributions, we compared MIRO-CO_2 simulations of seasonal evolution of pCO_2 and annual air-sea CO_2 fluxes in BCZ obtained by closing separately biological processes, *Phaeocystis* only and the river inputs of organic and inorganic carbon. A supplementary MIRO-CO_2 scenario with closing both biological processes and carbon river inputs was conducted to extract the solely thermodynamic effect of temperature change on pCO_2. For scenarios suppressing carbon river inputs, the river nutrient inputs to the BCZ were maintained.

Suppressing biological processes predicts in BCZ an important annual source of atmospheric CO_2 (+0.58 mol C m^{-2} y^{-1}, Fig. 5b). This suggests that biology is responsible of the annual sink predicted in BCZ (Fig. 5a) by taking up 0.75 mol C m^{-2} y^{-1} of atmospheric CO_2 Additional comparison with scenarios closing separately *Phaeocystis* colonies estimates at more than 50% the contribution of their bloom to this uptake

(−0.47 mol C m^{-2} y^{-1}, Fig. 5b). Suppression of river inputs of organic and inorganic carbon has no influence on the seasonal evolution of pCO_2 but increases significantly the annual CO_2 sink obtained with the reference run (Fig. 5a, c). Carbon river inputs thus represent a significant source of atmospheric CO_2 (+0.87 mol C m^{-2} y^{-1}) that is partly counteracted by biology on an annual scale (−0.75 mol C m^{-2} y^{-1}). Finally our scenarios predict an annual sink of atmospheric CO_2 of −0.33 mol C m^{-2} y^{-1} associated to the seasonal signal of the only temperature (Fig. 5d). All together these scenarios shows the predominance of different controls of pCO_2 and air-sea CO_2 exchanges in central BCZ along the season. Clearly carbon river inputs are responsible of the simulated emission of CO_2 to the atmosphere in late winter, counteracting the effect of cold temperature. Primary production, mostly that associated to *Phaeocystis* colonies explains the predicted CO_2 sink in spring which, under these conditions of temperature should have been a CO_2 source towards the atmosphere. During summer, temperature first and then C remineralization are the most important controls.

3.3 Role of land-based nutrients

In order to evaluate the role of land-based nutrients and carbon in modulating the seasonal cycle of surface water pCO_2 and air-sea CO_2 fluxes, we compared model results in central BCZ with those obtained for the WCH open-waters boundary conditions (Fig. 6). For this purpose simulations of pCO_2 (Fig. 6a) and air-sea CO_2 exchanges (Fig. 6b) in both areas were compared with the temperature forcing (Fig. 6c) and the simulated NEP (Fig. 6d). First of all, a fairly good agreement is observed between daily simulations of pCO_2 and available field data (Fig. 6a) in the WCH. As a general trend surface water pCO_2 in WCH is driven by temperature variation, being under-saturated with respect to the atmosphere between October and mid-March and super-saturated during spring-summer (Fig. 6a). Over the latter period, two small decreases in pCO_2 are simulated, coinciding with events of elevated NEP (Fig. 6d) that are reverting the effect of temperature increase (Fig. 6a, c, d). However and contrary to BCZ, the simu-

lated pCO_2 never reaches under-saturated values in spring due to the low productivity of WCH compared to BCZ (Fig. 6a). At the annual scale indeed BCZ is net autotrophic (integrated NEP=+0.2 g C m^{-2} y^{-1}) while WCH is close to metabolic balance (integrated NEP ~0 g C m^{-2} y^{-1}). Accordingly, WCH is almost in equilibrium with respect to atmospheric CO_2 (−0.01 mol C m^{-2} y^{-1}; Fig. 6b) when BCZ acts as a sink (−0.17 mol C m^{-2} y^{-1}).

Applying the Takahashi et al. (2002)'s approach to WCH simulations concludes that temperature variation over the year contributes more to pCO_2 seasonal variation than biology (T/B=1.21). Comparing this result with T/B obtained in BCZ (0.66) points the major contribution of rivers in counteracting the temperature control on surface water pCO_2.

3.4 Sensitivity to external present-day forcings

In this section we explore to what extent changing meteorological conditions (rainfall, temperature, wind stress) could alter the seasonal and annual dynamics of CO_2 in coastal waters. For this application, MIRO-CO_2 scenarios with changing nutrients and carbon river inputs, seawater temperature and wind speed forcings corresponding to two contrasted "meteorological" years (the dry 1996 and wet 1999 year) were run and compared. Over 1996–1999, nutrient loads were very variable, modulated by freshwater discharge that was higher in 1999 compared to 1996 (Rousseau et al., 2003; Fig. 7a). Nutrient concentrations in the Seine and Scheldt rivers were indeed unchanged over this period (Rousseau et al., 2003). Similarly, concentrations of organic and inorganic carbon were assumed constant. Significantly higher temperatures were observed in 1999 compared to 1996, especially between January and August (Fig. 7b). Daily wind speeds were quite variable with however similar annual averages of 5.05 and 5.16 m s^{-1} in 1996 and 1999, respectively (Fig. 7c).

The relative impact of external forcing variability was explored based on a comparison of modelled pCO_2 along the season (Fig. 8) and MIRO-CO_2 annual budget of biological activity (GPP, R and NEP) and air-sea CO_2 flux (Table 1). As general trend,

the seasonal trends and magnitude of pCO_2 variations were not significantly modified. However, significant changes in the intensity and direction of the annual air-sea CO_2 flux were calculated (Table 1).

3.4.1 Wind speed forcing

We found a negligible effect of wind speed on the pCO_2 annual cycle (Fig. 8a), since this forcing does not control NEP and temperature in our model. However, the daily variability of wind speed has a moderate impact on the air-sea CO_2 fluxes (Table 1). The largest sink is predicted in 1996 (−0.2 mol C m^{-2} y^{-1}, Table 1) and corresponds to lower gas transfer velocity, (8.38 and 8.58 cm h^{-1} (normalized to a Schmidt number of 600) in 1996 than in 1999, respectively).

3.4.2 River forcing

Comparison of pCO_2 simulations obtained with 1996 and 1999 river forcings, shows for 1996 lower values between January and March, similar in May and higher from May to August (Fig. 8b). The lower late winter pCO_2 simulated in 1996 are mostly due to the lower DIC river inputs as biological activity in winter is low. The initial winter pCO_2 value in 1996 also probably explains why spring minimal pCO_2 values are very similar for both years (Fig. 8b), although the maximum NEP value during the *Phaeocystis* bloom is higher in 1999 than 1996 (3.35 g C m^{-2} d^{-1} in 1999 compared to 2.57 g C m^{-2} d^{-1} in 1996, not shown).

On an annual base we calculated a lower sink for atmospheric CO_2 in 1999 compared to 1996 (Table 1) which contrasts with the elevated NEP simulated in 1999 (Table 1) in response to higher nutrient inputs. This has to be related to the higher DIC river inputs in 1999 that induce higher initial winter pCO_2 values (Fig. 8b). Altogether this scenario points the dual role of river inputs on the seasonal dynamics of pCO_2 in eutrophied coastal waters by modulating the carbon and nutrient conditions.

3.4.3 Temperature forcing

Clearly difference in timing and magnitude observed between surface water pCO_2 simulated in 1996 compared to 1999 (Fig. 8c) corresponds with temperature deviation mainly over January-to-July (Fig. 7b). Over this period temperature in 1999 is significantly higher than in 1996 (~3°C, Fig. 7b). In order to eliminate the temperature effect, modelled pCO_2 was normalized at the mean temperature of the BCZ (11.9°C, Fig. 8d). In January and early February, the lower pCO_2 values in 1996 are clearly due to lower temperatures compared to 1999 (Fig. 8). The offset of 9 days of the minimal simulated pCO_2 values, between 1996 and 1999 (Fig. 8), is related to a delay in 1996 of maximal *Phaeocystis* bloom as a consequence of the temperature dependence of GPP. On an annual base, NEP is lower in 1999 than in 1996 (Table 1), since higher GPP in 1999 than in 1996 (Table 1), due to the stronger dependence of R than GPP on temperature.

The shift from an annual sink in 1996 to a source in 1999 of atmospheric CO_2 (Table 1) is related to a combination of temperature effect on the carbon chemistry and biology (increased respiration at high temperature). Their relative importance can be assessed through the calculation of the T/B i.e. the ratio between $\Delta pCO_{2(temp)}$ and $\Delta pCO_{2(bio)}$ (Table 1). This suggests a higher temperature effect on biology than carbon chemistry. Indeed the T/B increases from 0.68 in 1996 to 0.69 in 1999 (Table 1) is because of a higher difference between $\Delta pCO_{2(bio)}$ (362 ppm in 1996 compared to 353 ppm in 1999) than $\Delta pCO_{2(temp)}$ (247 ppm in 1996 and 244 ppm in 1999).

4 Conclusions

The MIRO-CO_2 simulations, by showing stronger seasonal signals of pCO_2 and related air-sea CO_2 fluxes in the carbon and nutrient-enriched BCZ compared to more oceanic waters (WCH), is giving strong additional support to observation-based conclusions on the key role of coastal areas in the global carbon cycle (e.g. Frankignoulle and Borges, 2001a). We also demonstrated the advantage of model simulations and sensitivity

analysis for the identification of the major physical and biological mechanisms controlling the seasonal dynamics of surface water pCO_2 and their external forcing. In particular, we highlighted the significance of the *Phaeocystis* bloom in the spring-time drawn-down of atmospheric CO_2. The model also allowed to explore how the intensity and direction of the annual air-sea CO_2 flux was changed in relation to realistic variations of environmental forcings such as water temperature, fresh water discharge and wind speed.

Model results suggested that the seasonal variation of pCO_2 in the BCZ is strongly driven by nutrient-enriched biological activity in spring that counteracts the effect of temperature increase. On an annual scale, the solely river inputs of organic and inorganic carbon are driving a source of CO_2 of +0.87 mol C m^{-2} y^{-1} that is balanced by an atmospheric CO_2 uptake of −0.74 and −0.33 mol C m^{-2} y^{-1} due to nutrient stimulated NEP and temperature change, respectively. Globally an annual weak sink is predicted for BCZ. However, based on a sensitivity analysis, we also showed that the present-day interannual variations of fresh water discharge (and related land-based nutrient and carbon inputs) and water temperature might have a significant impact on the air-sea CO_2 fluxes in the BCZ.

These simulations clearly illustrate the potentially significant but complex variations of CO_2 fluxes in near-shore coastal ecosystems in response to small environmental changes within the range of present-day variability. These variations in CO_2 fluxes are a small glimpse of those that can be expected from environmental changes predicted in the near future in context of global change and/or of management strategies.

Acknowledgements. This work was carried out in the framework of the Belgium Federal Science Policy projects AMORE (EV/11/19) and CANOPY (EV/03/20), the EU-FP5 project EUROTROPH (EVK3-CT-2000-00040) and the project 2.4545.02 of the Fonds National de la Recherche Scientifique (FNRS). DIC and TA data in the Seine estuary were kindly provided by G. Abril (Département de Géologie et Océanographie, Université de Bordeaux 1). A. V. Borges is a FNRS post-doctoral researcher. N. Gypens has financial support from the 'Fond pour la Formation à la Recherche dans l'Industrie et dans l'Agriculture' (FRIA, FNRS, Belgium).

References

Billen, G. and Servais, P.: Modélisation des processus de dégradation bactérienne de la matière organique en milieu aquatique, edited by Bianchi et coll: Micro-organismes dans les écosystèmes océaniques, Masson, 219–245, 1989.

Borges, A. V. and Frankignoulle, M.: Daily and seasonal variations of the partial pressure of CO_2 in the surface seawater along Belgian and southern Dutch coastal areas, J. Mar. Syst., 19, 251–266, 1999.

Borges, A. V. and Frankignoulle, M.: Distribution of surface carbon dioxide and air-sea exchange in the upwelling system off the Galician coast, Global Biogeochem. Cycles, 16(2), 1020, 2002a.

Borges, A. V. and Frankignoulle, M.: Distribution and air-water exchange of carbon dioxide in the Scheldt plume off the Belgian coast, Biogeochemistry, 59, 41–67, 2002b.

Borges, A. V. and Frankignoulle, M.: Distribution of surface carbon dioxide and air-sea exchange in the English Channel and adjacent areas, J. Geophys. Res., 108(C8), 3140, doi:10.1029/2000JC000571, 2003.

Borges, A. V., Djenidi, S., Lacroix, G., Théate, J.-M., Delille, B., and Frankignoulle, M.: CO_2 atmospheric flux from mangrove surrounding waters, Geophys. Res. Let., 30(11), 1558, doi:10.1029/2003GL017143, 2003.

Bouillon, S., Frankignoulle, M., Dehairs, F., Velimirov, B., Eiler, A., Abril, G., Etcheber, H., and Borges, A. V.: Inorganic and organic carbon biogeochemistry in the Gautami Godavari estuary (Andhra Pradesh, India) during pre-monsoon: the local impact of extensive mangrove forests, Global Biogeochem. Cycles, 17 (4), 1114, doi:10.1029/2002GB002026, 2003.

Brasse, S., Nellen, M., Seifert, R., and Michaelis, W.: The carbon dioxide system in the Elbe estuary, Biogeochemistry, 59(1–2), 25–40, 2002.

Cai, W. J., Wiebe, W. J., Wang, Y. C., and Sheldon, J. E.: Intertidal marsh as a source of dissolved inorganic carbon and a sink of nitrate in the Satilla River-estuarine complex in the southeastern US, Limnol. Oceanogr., 45(8), 1743–1752, 2000.

Cai, W.-J., Wang, Z. A., and Wang, Y.: The role of marsh-dominated heterotrophic continental margins in transport of CO_2 between the atmosphere, the land-sea interface and the ocean, Geophys. Res. Lett., 30, 3-1/3-4, 2003.

DeGrandpre, M. D., Olbu, G. J., Beatty, C. M., and Hammar, T. R.: Air-sea CO_2 fluxes on the US Middle Atlantic Bight, Deep-Sea Research Part Ii-Topical Studies in Oceanography, 49(20),

4355–4367, 2002.

Frankignoulle, M. and Borges, A. V.: European continental shelf as a significant sink for atmospheric carbon dioxide, Global Biogeochem. Cycles, 15(3), 569–576, 2001a.

Frankignoulle, M. and Borges, A. V.: Direct and indirect pCO_2 measurements in a wide range of pCO2 and salinity values (the Scheldt estuary), Aquatic Geochemistry, 7, 267–273, doi:10.1023/A:1015251010481, 2001b.

Frankignoulle, M., Bourge, I. and Wollast, R.: Atmospheric CO_2 fluxes in a highly polluted estuary (The Scheldt), Limnology and Oceanography, 41(2), 365–369, 1996.

Frankignoulle, M., Abril, G., Borges, A. V., Bourge, I., Canon, C., Delille, B., Libert, E., and Théate, J.-M.: Carbon dioxide emission from European estuaries, Science, 282, 434–436, 1998.

Gattuso, J.-P., Frankignoulle, M., and Wollast, R.: Carbon and carbonate metabolism in coastal aquatic ecosystems, Ann. Rev. Ecol. Syst., 29, 405–433, 1998.

Hannon, E., Boyd, P. W., Silvoso, M., and Lancelot, C.: Modelling the bloom evolution and carbon flows during SOIREE: Implications for future in situ iron-experiments in the Southern Ocean, Deep-Sea Research II, 48, 2745–2773, 2001.

Hoppema, J. M. J.: The seasonal behaviour of carbon dioxide and oxygen in the coastal North Sea along the Netherlands, Netherlands Journal of Sea Research, 28(3), 167–179, 1991.

Ianson, D. and Allen, E.: A two-dimensional nitrogen and carbon flux model in a coastal upwelling region, Global Biogeochem. Cycles, 6 (1), 1011, doi:10.1029/2001GB0001451, 2002.

Kaul, L. and Froelich, P.: Modelling estuarine nutrient biogeochemistry in a simple system, Geochim. Cosmochim. Acta, 48, 1417–1433, 1984.

Lancelot, C.: The mucilage phenomenon in the continental coastal waters of the North Sea, The Science of the Total Envir., 165, 83–102, 1995.

Lancelot, C., Billen, G., Sournia, A., Weisse, T., Colijn, F., Veldhuis, M., Davies, A., and Wassmann, P.: *Phaeocystis* blooms and nutrient enrichment in the continental coastal zone of the North Sea, Ambio, 16(1), 38–46, 1987.

Mackenzie, F. T., Lerman, A., and Andersson, A. J.: Past and present of sediment and carbon biogeochemical cycling models, Biogeosciences, 1, 11–32, 2004, SRef-ID: 1726-4189/bg/2004-1-11.

Millero, F. J., Zhang, J.-Z., Fiol, S., Sotolonge, S., Roy, R. N., Lee, K., and Mane, S.: The use of buffers to measure pH in seawater, Marine Chemistry, 44, 143–152, 1993.

Nightingale, P. D., Malin, G., Law, C. S., Watson, A. J., Liss, P. S., Liddicoat, M. I., Boutin, J., and Upstill-Goddard, R. C.: In-situ evaluation of air-sea gas exchange parametrizations using novel conservative and volatile tracers, Global Biogeochem. Cycles, 14, 373–387, 2000.

Raymond, P. A., Bauer, J. E., and Cole, J. J.: Atmospheric CO_2 evasion, dissolved inorganic carbon production, and net heterotrophy in the York River estuary, Limnol. Oceanogr., 45(8), 1707–1717, 2000.

Rousseau, V.: Dynamics of *Phaeocystis* and diatom blooms in the eutrophicated coastal waters of the Southern Bight of the North Sea, PhD Thesis, Université Libre de Bruxelles, Belgium, 205, 2000.

Rousseau, V., Breton, E., De Wachetr, B., Beji, A., Deconinck, M., Huijgh, J., Bolsens, T., Leroy, D., Jans, S., and Lancelot, C.: Identification of Belgian maritime zones affected by eutrophication (IZEUT): Towards the establishment of ecological criteria for the implementation of the OSPAR Common Procedure to combat eutrophication, Belgian Science Policy publisher, in press, 100, 2004.

Takahashi, T., Sutherlan, S. C., Sweeney, C., Poisson, A., Metzl, N., Tilbrook, B., Bates, N., Wanninkhof, R., Feely, R. A., Sabine, C., Olafsson, J., and Nojiri, Y.: Global sea-air CO_2 flux based on climitalogical surface ocean pCO_2, and seasonal biological and temperature effects, Deep-sea Research II, 49, 1601–1622, 2002.

Takahashi, T., Sutherland, S. C., Feely, R. A., and Cosca, C. E.: Decadal variation of the surface water pCO_2 in the western and central equatorial Pacific, Science, 302(5646), 852–856, 2003.

Servais, P., Mercier P., and Anzil, A.: Activité hétérotrophe et biodégradabilité de la matière organique dans la zone de turbidité maximale de l'estuaire de Seine, Programme Seine-Aval, 2003.

Thomas, H., Bozec, Y., Elkalay, K., and de Baar, H. J. W.: Enhanced open ocean storage of CO_2 from shelf sea pumping, Science, 304, 1005–1008, 2004a.

Thomas, H., Bozec, Y., de Baar, H., Elkalay, K., Frankignoulle, M., Schiettecatte, L.-S., and Borges, A. V.: The Carbon budget of the North Sea, Biogeosciences Discussions, 367–392, 2004b.

Tsunogai, S., Watanabe, S., and Sato, T.: Is there a "continental shelf pump" for the absorption of atmospheric CO_2?, Tellus Series B-Chemical and Physical Meteorology, 51(3), 701–712, 1999.

Walsh, J. J. and Dieterle, D. A.: CO_2cycling in the coastal ocean, I. – A numerical analysis of

the Southeastern Bering Sea with applications to the Chukchi Sea and the northern Gulf of Mexico, Prog. Oceanog., 34, 335–392, 1994.

Walsh, J. J., Dieterle, D. A., Muller-Karger, F. E., Aagaard, K., Roach, A. T., Whitledge, T. E., and Stockwell, D.: CO_2 cycling in the coastal ocean, II. Seasonal organic loading of the Arctic Ocean from source waters in the Bering Sea, Cont. Shelf Res., 17(1), 1–36, 1996.

Wang, Z. A. and Cai, W.-J.: Carbon dioxide degassing and inorganic carbon export from a marsh-dominated estuary (the Duplin River): A marsh CO_2 pump, Limnol. Oceanogr., 49(2), 341–354, 2004.

Weiss, R. F.: Carbon dioxide in the water and seawater: the solubility of a non-ideal gas, Marine Chemistry, 2, 203–205, 1974.

Table 1. Comparison between annually-integrated air-sea CO_2 fluxes, gross primary production (GPP), respiration (R) and net ecosystem production (NEP) computed for the reference run (1996–1999) and with separate 1996 and 1999 river, temperature and wind speed forcing. The relative importance of temperature and biology effect on pCO_2 is expressed by the ratio T/B.

	Reference	Wind speed		River discharge		Temperature	
	1996–1999	1996	1999	1996	1999	1996	1999
Air-sea CO_2 flux, molC m^{-2} y^{-1}	−0.17	−0.20	−0.14	−0.24	−0.05	−0.39	+0.04
GPP, gC m^{-2} y^{-1}	225	225	225	206	263	206	237
R, gC m^{-2} y^{-1}	221	221	221	202	257	200	232
NEP, gC m^{-2} y^{-1}	+4.6	+4.6	+4.6	+3.9	+6.7	+5.3	+5.0
T/B	0.66	0.66	0.65	0.68	0.6	0.68	0.69

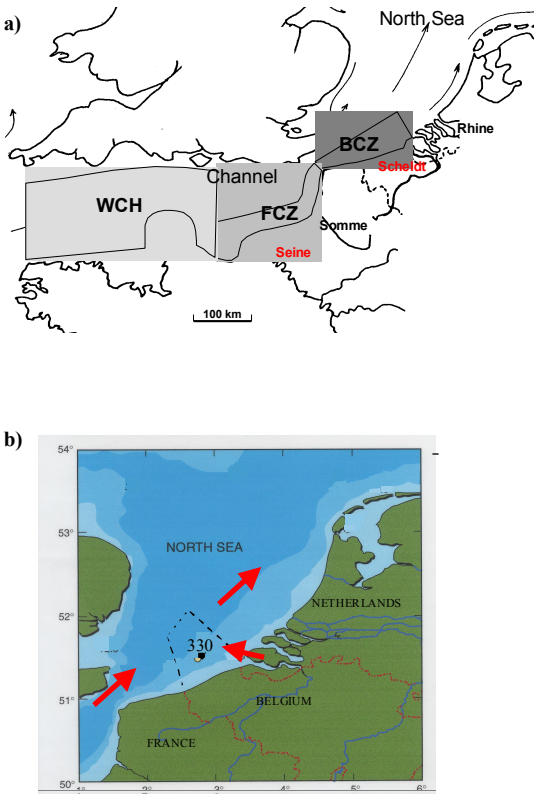

Fig. 1. Map of the studied area showing **(a)** the MIRO multi-box frame (adapted from Lancelot et al., in review, 2004[1]) and **(b)** the location of the station 330 (51°26.05′ N; 002°48.50′ E).

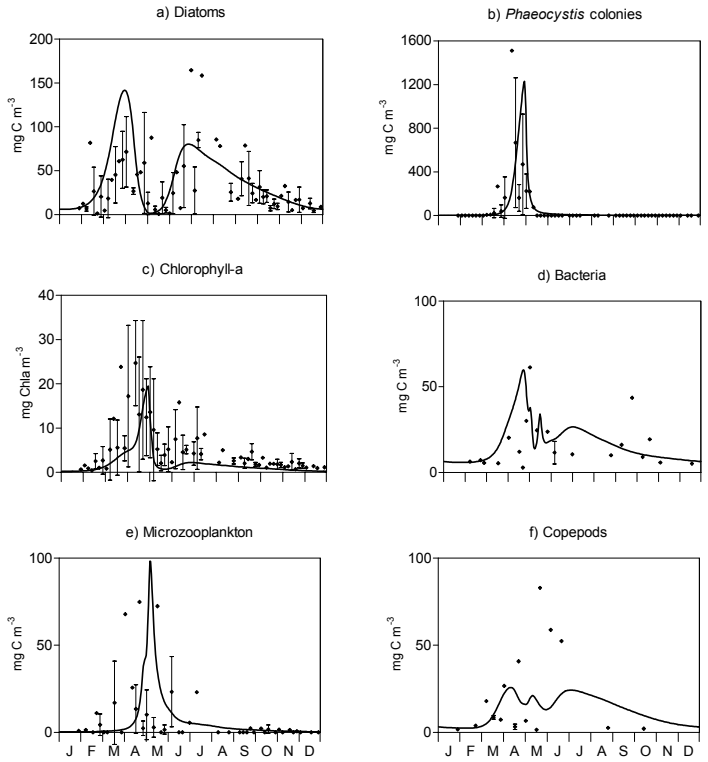

Fig. 2. Model results (solid line) and observations (◊) of **(a)** diatoms, **(b)** *Phaeocystis* colonies, **(c)** Chlorophyll-a, **(d)** bacteria, **(e)** microzooplankton and **(f)** copepods at the station 330 for the 1996–1999 period.

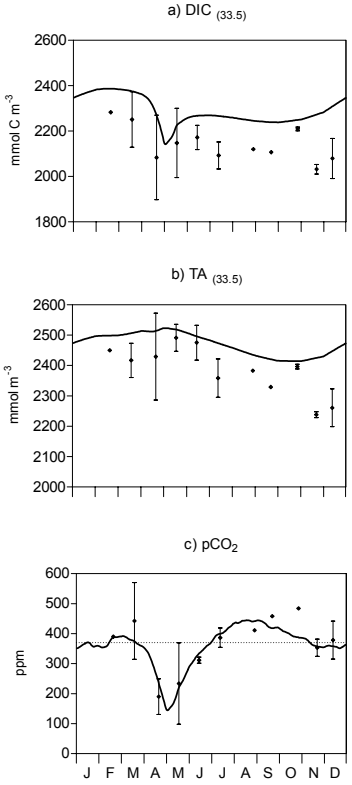

Fig. 3. Model results (solid line) and observations (◊) of **(a)** dissolved inorganic carbon $DIC_{(33.5)}$, **(b)** total alkalinity $TA_{(33.5)}$and **(c)** surface water pCO_2. The dotted line corresponds to the atmospheric equilibrium.

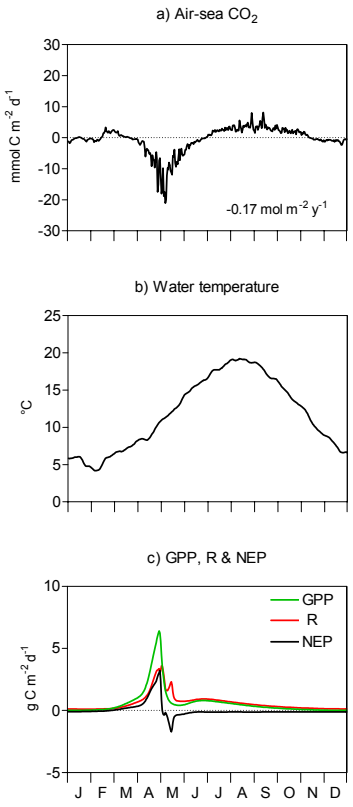

Fig. 4. Seasonal evolution of modelled **(a)** air-sea CO_2 flux, **(b)** mean water temperature for the 1996–1999 period and **(c)** gross primary production (GPP), total respiration (R) and net ecosystem production (NEP) computed for BCZ.

585

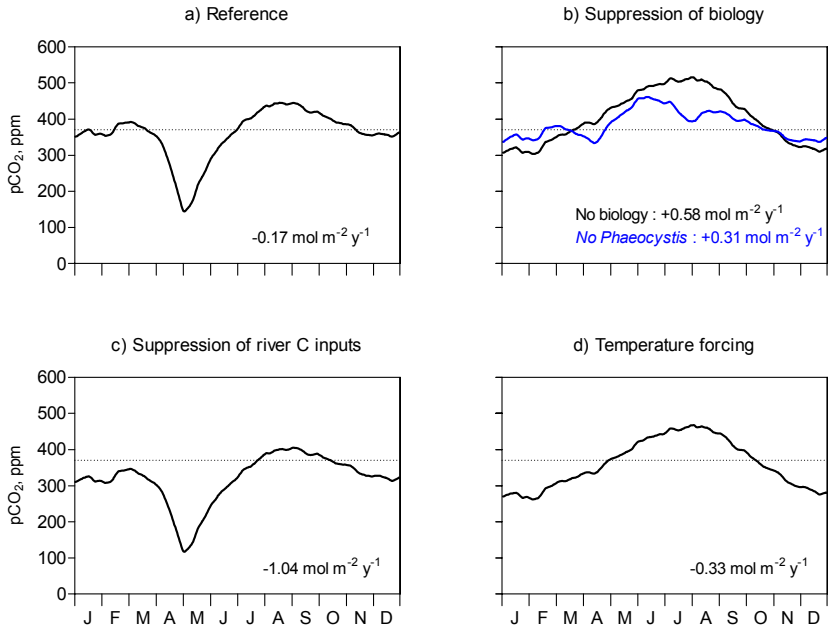

Fig. 5. Seasonal evolution of pCO_2 computed for **(a)** the reference run and by closing **(b)** biological processes or only *Phaeocystis* growth, **(c)** inorganic and organic carbon river inputs or **(d)** both biological processes and carbon inputs. The annual integrated CO_2 air-sea flux computed for each scenario is indicated on the corresponding plot.

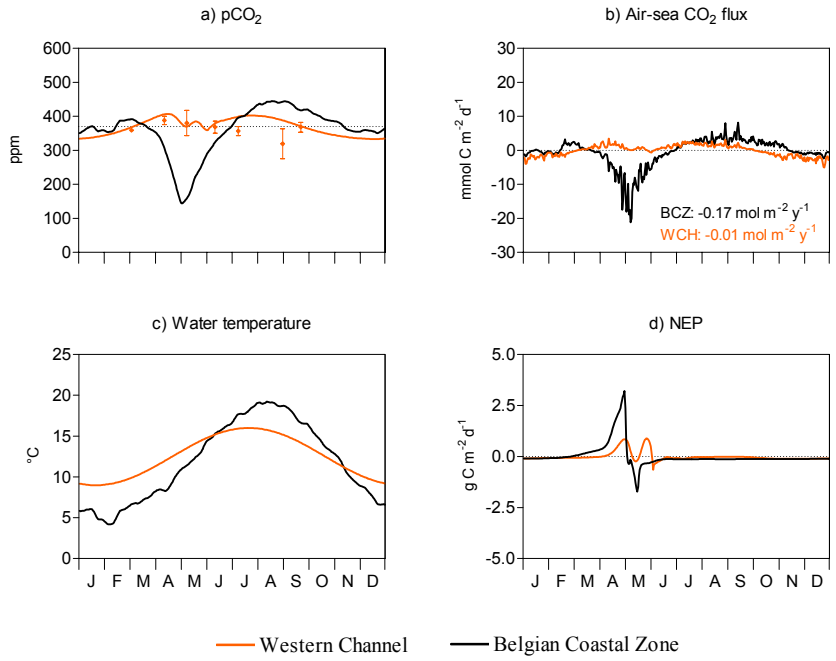

Fig. 6. Seasonal evolution of daily modelled **(a)** pCO_2, **(b)** air-sea CO_2 flux, **(c)** water temperature and **(d)** net ecosystem production computed for WCH and BCZ boxes. Model results of pCO_2 in WCH (solid line) are compared with available observations in that area (◇). The dotted line, in the pCO_2 plots, corresponds to atmospheric pCO_2. The calculated annual CO_2 air-sea flux is added to each plot of air-sea CO_2 flux.

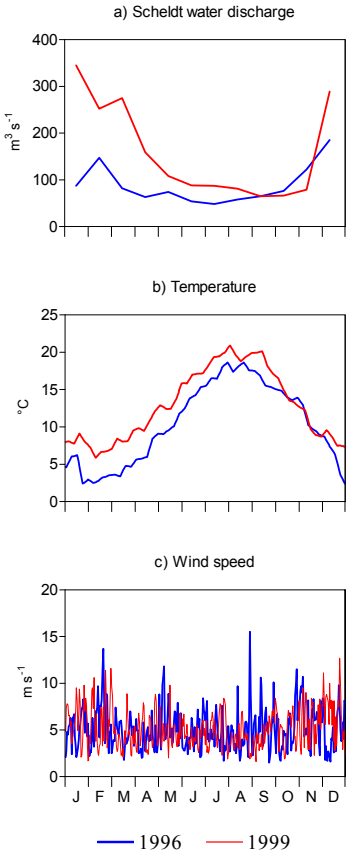

Fig. 7. Seasonal cycle of **(a)** Scheldt fresh water discharge, **(b)** water temperature and **(c)** wind speed for 1996 and 1999.

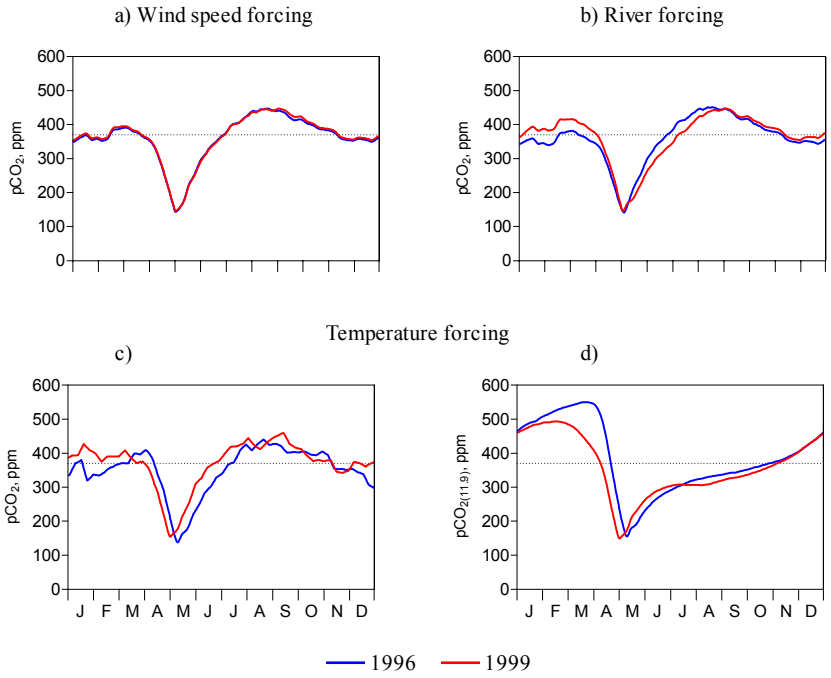

Fig. 8. Seasonal evolution of modelled pCO_2 computed with **(a)** wind speed forcing, **(b)** river **(c)** temperature forcings of 1996 and 1999 and **(d)** same as (c) but normalized to BCZ average temperature of 11.9°C. The dotted line corresponds to atmospheric equilibrium.